Equation of state and sound speed of cesium at temperatures up to 2200 K and pressures up to 60 MPa

V. F. Kozhevnikov

Moscow Aviation Institute
(Submitted 29 June 1989)
Zh. Eksp. Teor. Fiz. **97**, 541–558 (February 1990)

Results are presented of measurements of the equation of state and speed of sound in cesium. The equation of state was measured at temperatures up to 2200 K and pressures up to 60 MPa in the liquid and vapor phases, including the coexistence curves as far as the critical point, and in the supercritical region; the error in the density data varied from 0.2 to 1.0 percent. The critical parameters of cesium were found to be 1938 K, 9.4 MPa, and 0.39 g cm^{-3}. The sound speed was measured to within 0.5–0.6% in the liquid phase up to temperatures of 2000 K and pressures of 60 MPa. Tables of the thermal and specific heat properties of liquid cesium in this parameter range have been complied. Questions relating to the shape of the coexistence curve, the average diameter, and the specific heat at constant volume are discussed. The critical region in cesium is shown to be two orders of magnitude smaller than in dielectrics.

1. INTRODUCTION

Cesium is one of the few metals for which the critical point for the gas-vapor phase transition is accessible to measurement under steady conditions; only mercury has a lower critical temperature.[1] At the same time, the relatively uncomplicated structure of the electronic spectrum of cesium enables us to use it as a standard against which to test theoretical models of metallic liquids. Insufficient experimental information is available in the literature, however, to permit us to draw a complete picture of the thermodynamic and specific-heat properties of cesium at high temperatures and to establish the properties of the liquid-metal state for comparison with nonconducting liquids. Therein lies the aim of the present work.

In Sec. 2 we describe the techniques employed in carrying out measurements of the equation of state (EOS) and the results obtained at temperatures up to 2200 K and pressures up to 60 MPa, spanning the liquid and vapor phases together with the coexistence curve and the supercritical region. In Sec. 3 we describe the techniques employed and the results obtained in carrying out measurements of the speed of sound at temperatures up to 2000 K and pressures up to 60 MPa. In Sec. 4 tables are presented of the thermodynamic properties of cesium: the density ρ, the thermal expansion coefficient $\alpha = -\rho^{-1}(\partial\rho/\partial T)_P$, the isothermal compressibility $k_T = \rho^{-1}(\partial\rho/\partial P)_T$, the sound speed U, the adiabatic compressibility $k_S = \rho^{-1}(\partial\rho/\partial T)_S$, the specific heats C_P and C_V, and their ratio $\gamma = C_P/C_V$. Discussion and conclusions are presented in Secs. 5 and 6, respectively.

2. EQUATION OF STATE

Table I summarizes the results of earlier measurements[1–11] of the critical parameters of cesium. The data obtained prior to 1975 are completely consistent. This might convey the impression that nothing further remains to be done in this field. But an examination of the methods used and the results obtained in those studies (see, e.g., Ref. 12) leads one to conclude that more accurate experiments are needed.

In the present work the EOS was measured using an airtight two-zone dilatometer, shown in Fig. 1. A thin-walled bellows made of stainless steel served as the elastic element, which allowed us to carry out measurements not only for the liquid phase, as was done in our previous work,[13] but also for the gas, including the saturation curve.

The cesium was 99.99% pure. The measuring element was filled with cesium in a vacuum of better than 5×10^{-5} Torr. The dilatometer was situated in a high-pressure bomb divided into cold and hot zones. The medium used to transmit pressures was argon. The pressure drop at the dilatometer was shown by calibration[14] to be less than 20 kPa for a volume change of 2.2 cm^3. The cell volumes we used varied from 1.7 to 2.0 cm^3.

The heater was made of two thin-walled coaxially fastened tungsten tubes 250 mm in length. At every experimental point the heater power was stabilized by means of a thyristor temperature regulator. The cell temperature distribution was held uniform by means of guard heaters which kept the temperature gradient $\Delta T/T$ along the cell below 10^{-3}. A detailed description of the experimental apparatus was given by Kozhevnikov and Ermilov.[15]

We used cells made of molybdenum and tungsten. The tungsten cell shown in Fig. 1 was made by precipitation from the gaseous phase of WF_6. In every case the ratio of the capillary volume to that of the cell was $\sim10^{-2}$. The mass of the cesium in the capillary was corrected by assuming a linear longitudinal temperature distribution. Other corrections were carried out as described in Ref. 13.

Figure 2 displays experimental data. The measurements were carried out along an isobar as the temperature increased and decreased. Over 600 experimental points were obtained. At pressures above 12 MPa the results agreed well with those of Ref. 13; the 30-MPa and 59-MPa isobars shown were constructed using the results of Ref. 13.

The liquid–vapor transition temperature was found to within an accuracy of ≈1 K (associated with the scale of the thermometer used) from the discontinuity in the sample density associated with heating and cooling. The values obtained for the boiling and condensation temperatures at pressures from 3 to 9 MPa agreed well (to within 1–3 K) with the elasticity curve for cesium vapor.[16] On the 0.9-MPa isobar boiling occurred with superheating sometimes reaching 60 K. There was no detectable recooling during condensation. At pressures above 9 MPa the experimental isobars

 0038-5646/90/020298-13$03.00

TABLE I. Critical parameters of cesium.

Measured quantity	Method	T_c, K	10^{-6} P_c, Pa	10^{-3} ρ, kg m^{-3}	Source
ρ_L, ρ_V (in the saturated state)	Electrical resistance	2027	–	0.445	[2]
ρ_L, ρ_V	Radioactive isotope	2057±40	147±30	0,428±0,012	[3]
P_s–T_s	From change in electrical conductivity	2023±30	110±10	–	[4]
ρ_L, ρ_V	Radioactive isotope	2033±20	116±5	0.40±0,02	[5]
ρ_L, ρ_V	»	2053±20	118±10	0.44±0.05	[6]
P_s–T_s	Boiling points	2050±3	116±0,5	–	[7]
ρ_L, ρ_V (in the saturated state)	Tilting capsule	2045±5	–	0.406	[8]
ρ_L, ρ_V (in the saturated state)	»	2048±0.6	117±0,2	0.42±0.02	[9]
ρ_L	Two-zone dilatometer	2013±20	113±1	0.41±0.02	[10]
P–T (at constant volume)	Two-zone constant-volume piezometer	1924	92,5	0.379	[11]
ρ_L, ρ_V (including the saturation curve)	Two-zone dilatometer	1938±10	94±2	0.39±0.01	Present work*

*Results first presented at session of USSR Academy of Sciences Scientific Council on "Physics of Highly Collisional Plasmas" (1986).

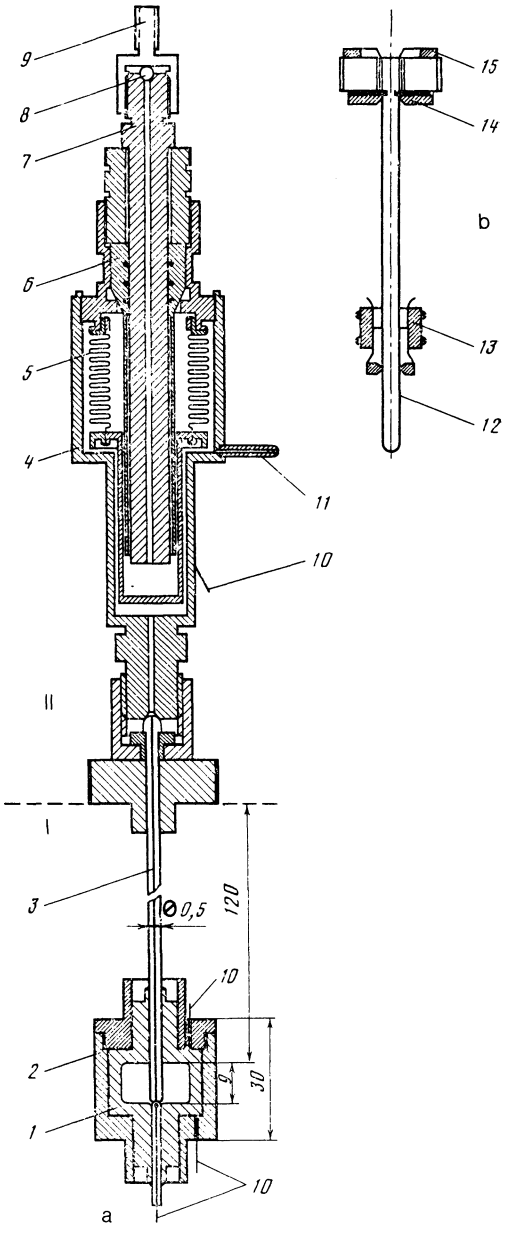

FIG. 1. Dilatometer: 1—cell (W or Mo); 2—container (Mo); 3—capillary (W or Mo); 4—body of measuring element; 5—bellow; 6, 7—pair of pistons; 8—plug of opening for refilling with mercury; 9—place for attaching slide for slide wire; 10—thermocouple; 11—tube for inserting cesium; 12—mast for slide wire; 13—slide wire with contacts; 14—stationary potential contacts; 15—elastic current-conducting contacts; I—hot zone; II—cold zone.

assume the smooth form typically observed in supercritical states.

Figure 2 also gives the values of the saturated vapor density taken from Vargaftik *et al.*,[17] which agree with the present data at temperatures up to 1800 K. In this comparison the low-pressure region, where the data of Ref. 17 are most reliable and where our experimental error is greatest, is of prime importance; at 1300 K the discrepancy is less than 1%. The same figure also shows experimental results[11] in satisfactory agreement with ours. It should be noted that Ref. 11 employed a different measurement technique: the values of the density on the saturation curve were found from the intersection of the experimental isochores and the saturated-vapor elasticity curve.

The relative error in our determination of the density, which varied by two orders of magnitude in the course of the experiments, ranged from 0.2% in the dense liquid to 1.0% in the rarefied gas.

The temperature of the sample was measured by three VR 5/20 tungsten-rhenium thermocouples prepared from one pair of calibrated wire coils. The absolute error in the temperature measurements varied form 5 K at $T \approx 1300$ K to 10 K at $T \approx 2100$ K. The error in the differential readings of the thermocouple was less than 1 K. The pressure was regulated with standard pressure gauges to within 20 kPa for $P \leqslant 10$ MPa and to within 0.1 MPa for $P > 10$ MPa.

The location of the critical point was determined from the intersection of the coexistence curve and the average diameter of the phase diagram. The critical parameters were $T_c = 1938 \pm 10$ K, $P_c = 9.4 \pm 0.2$ MPa, and $\rho_c = 0.39 \pm 0.1$ g cm^{-3}. These values of the critical parameters differ considerably from most of those found in earlier work, but agree with the most recent results found by Hensel's group[12] (cf. Table I).

3. SPEED OF SOUND

The speed of sound in liquid cesium has been studied experimentally on the saturation curve in six papers (reviewed by Novikov *et al.*[18]). The maximum temperature reached in these studies[19] was 1100 K; $U(T)$ was presented by a linear approximation.

In the present work the speed of sound was measured with apparatus described previously.[20] The pulsed-phase technique on which it is based permits the sound propagation time to be measured to within 1 ns. The need for such great precision arises because at these high temperatures and pressures one has to deal with samples ~ 1 mm in dimension, a factor of ten smaller than the usual sample in liquid-metal experiments.

The measuring element in this work was made from a molybdenum tube; the soundguide and limiting ring were also made the molybdenum. The pressure load on the airtight cell was applied by means of a bellows spreader baked onto the molybdenum tube. In the experiments we measured the change in the sound propagation time through the tube as a function of temperature and pressure relative to a reference state, a specified as 305 K and atmospheric pressure. The speed of sound there was taken to be $U_0 = 958$ m s^{-1} (Ref. 18).

Taking into account thermal expansion of the molybdenum and the errors in the published value of U_0, we conclude that the error in our values of the sound speed was 0.5–0.6%. The temperature and pressure were measured with the same instrumentation as in the EOS experiments.

The measurements were carried out at a frequency of approximately 10 MHz on an isobar under steady conditions, with automatic checking of reproducibility as the temperature increased and decreased. Over 300 experimental points were obtained, some of which are shown in Fig. 3. Seven sizes of measuring cells were used, ranging from 2 to 4 mm. The resulting data agreed well with the results of our previous series of experiments, in which the sound speed was measured for $T \leqslant 1400$ K and $P \leqslant 60$ MPa in a stainless steel cell.[21] The experimental results also agreed with those of Novikov *et al.*,[19] except that, as can be seen from Fig. 3, the

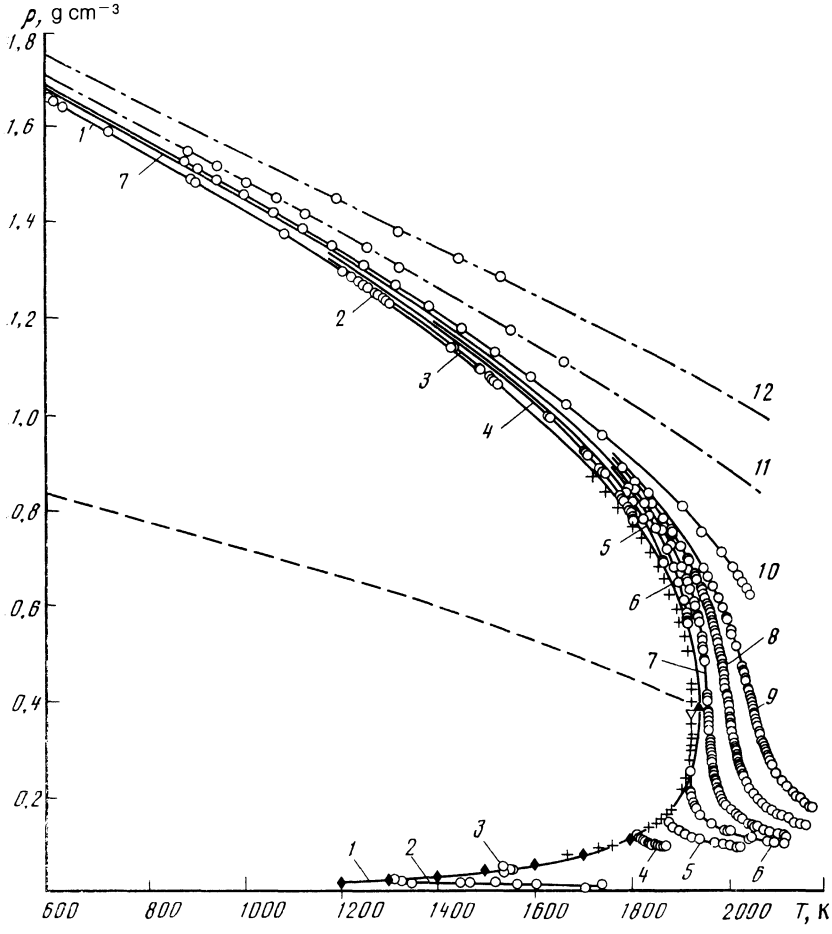

FIG. 2. Equation of state of cesium (experimental data): 1 is the coexistence curve; 2–12 correspond to the following values of P in MPa: 2—0.98, 3—3.04; 4—6.96; 5—7.94; 6—8.92; 7—9.90; 8—10.7; 9—11.9; 10—14.8; 11—29.5; 12—58.9; ▲ indicates the critical point, ♦ the density of the saturated vapor,[17] + the density of coexisting liquid and vapor, and ▽ the critical point from Ref. 11.

temperature dependence of the sound speed departed from linearity for $T \geqslant 900$ K.

The highest temperatures (around 2000 K) were attained at high pressures. The maximum temperature measured on the saturation curve was 1700 K and was accompanied by a substantial decrease in the wave resistance of the sample relative to the impedance of the soundguide at high temperatures.

4. THERMODYNAMIC PROPERTIES OF LIQUID CESIUM

In order to calculate the thermodynamic and specific heat properties of cesium we have to take derivatives of the density with respect to temperature and pressure. This is typically done by fitting the data with some analytic function. The effectiveness of such a procedure depends in large measure on whether there is any theoretical justification for

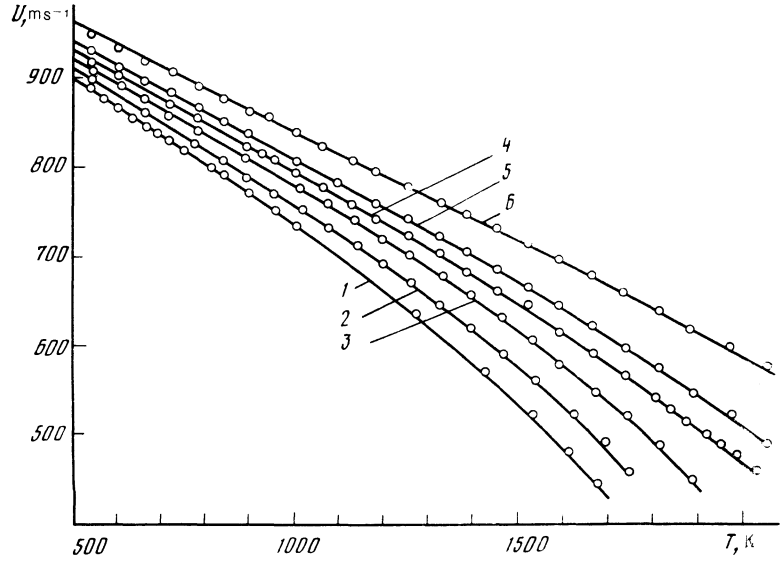

FIG. 3. Speed of sound in liquid cesium: 1—on the saturation curve; 2—for $P = 9.9$ MPa; 3—for $P = 19.7$ MPa; 4—for $P = 29.5$ MPa; 5—for $P = 39.3$ MPa; 6—for $P = 58.9$ MPa.

TABLE II. Thermodynamic properties of liquid cesium.

$P\cdot10^{-5}$, Pa	$\rho\cdot10^{-3}$, kg m^{-3}	$\alpha_P\cdot10^{3}$, K^{-1}	$k_T\cdot10^{9}$, Pa^{-1}	U, m s	$k_S\cdot10^{9}$, Pa^{-1}	C_P, J kg^{-1}K^{-1}	C_V, J kg^{-1}K^{-1}	γ
			T=400 K					
0	1.781	0.32	0.74	930	0.65	228	197	1.15
50	1.787	0.32	0.73	–	–	–	–	–
100	1.794	0.31	0.72	–	–	–	–	–
200	1.806	0.30	0.71	–	–	–	–	–
300	1.818	0.29	0.69	–	–	–	–	–
400	1.830	0.29	0.67	–	–	–	–	–
600	1.854	0.27	0.63	–	–	–	–	–
			T=500 K					
0.0	1.723	0.33	0.86	898	0.72	228	191	1.19
50	1.730	0.32	0.84	903	0.71	227	191	1.19
100	1.738	0.32	0.83	908	0.70	226	191	1.18
200	1.752	0.31	0.80	919	0.68	226	191	1.18
300	1.765	0.30	0.77	930	0.66	225	192	1.18
400	1.778	0.30	0.75	940	0.64	225	192	1.17
600	1.804	0.28	0.70	960	0.60	224	192	1.17
			T=600 K					
0.01	1.666	0.34	0.99	866	0.80	227	184	1.23
50	1.674	0.33	0.96	872	0.78	226	184	1.22
100	1.682	0.33	0.94	878	0.77	225	185	1.22
200	1.697	0.32	0.90	891	0.74	224	185	1.21
300	1.712	0.31	0.86	903	0.72	223	185	1.21
400	1.726	0.30	0.83	914	0.69	223	186	1.20
600	1.754	0.29	0.78	935	0.65	222	186	1.19

Table II. (cont.).

$P\cdot10^{-5}$, Pa	$\rho\cdot10^{-3}$, kg m^{-3}	$\alpha_P\cdot10^{3}$, K^{-1}	$k_T\cdot10^{9}$, Pa^{-1}	U, m s^{-1}	$k_S\cdot10^{9}$, Pa^{-1}	c_P, J kg^{-1}K^{-1}	c_V, J kg^{-1}K^{-1}	γ
				T=700 K				
0.05	1.609	0.35	1.14	835	0.89	225	177	1.27
50	1.617	0.34	1.10	841	0.87	224	177	1.26
100	1.626	0.34	1.07	848	0.85	223	178	1.26
200	1.643	0.33	1.02	862	0.82	222	178	1.25
300	1.659	0.32	0.98	875	0.79	222	179	1.24
400	1.675	0.31	0.94	887	0.76	221	179	1.24
600	1.704	0.29	0.87	911	0.71	220	180	1.23
				T=800 K				
0.21	1.552	0.37	1.31	803	1.00	225	171	1.31
50	1.561	0.36	1.27	811	0.97	223	171	1.30
100	1.571	0.35	1.23	818	0.95	222	172	1.30
200	1.588	0.34	1.16	834	0.90	221	172	1.29
300	1.605	0.33	1.11	848	0.87	221	173	1.28
400	1.622	0.32	1.06	861	0.83	220	173	1.27
600	1.654	0.30	0.97	886	0.77	219	174	1.26
				T=900 K				
0.67	1.494 / 0.001	0.39	1.54	770	1.13	224	164	1.37
50	1.505	0.38	1.49	779	1.09	223	164	1.36
100	1.515	0.37	1.43	788	1.06	222	165	1.35
200	1.533	0.36	1.34	806	0.98	221	166	1.33
300	1.552	0.34	1.27	821	0.95	220	166	1.32
400	1.570	0.33	1.20	835	0.91	220	167	1.31
600	1.604	0.31	1.09	862	0.84	218	168	1.30
				T=1000 K				
1.7	1.435 / 0.003	0.43	1.85	735	1.29	225	157	1.43
50	1.446	0.41	1.76	746	1.24	223	158	1.42
100	1.457	0.40	1.68	757	1.20	222	158	1.40
200	1.477	0.38	1.55	778	1.12	220	159	1.39
300	1.497	0.36	1.45	795	1.06	219	160	1.37
400	1.516	0.35	1.37	810	1.01	218	160	1.36
600	1.554	0.32	1.23	838	0.92	216	162	1.34

Table II. (cont.).

$P\cdot10^{-5}$, Pa	$\rho\cdot10^{-3}$, kg m^{-3}	$\alpha_P\cdot10^{3}$, K^{-1}	$k_T\cdot10^{9}$, Pa^{-1}	U, m s^{-1}	$k_S\cdot10^{9}$, Pa^{-1}	c_P, J kg^{-1} K^{-1}	c_V, J kg^{-1} K^{-1}	γ
				T=1100 K				
3.6	1.373 / 0.006	0.47	2.26	698	1.49	228	151	1.51
50	1.385	0.45	2.13	711	1.43	226	152	1.49
100	1.397	0.43	2.01	724	1.37	224	152	1.47
200	1.419	0.40	1.81	749	1.26	221	153	1.44
300	1.441	0.38	1.67	767	1.18	219	154	1.42
400	1.463	0.36	1.56	783	1.11	217	155	1.40
600	1.504	0.33	1.38	814	1.00	216	157	1.37
				T=1200 K				
6.9	1.308 / 0.011	0.53	2.85	660	1.76	237	146	1.62
50	1.321	0.49	2.62	675	1.66	231	146	1.58
100	1.335	0.47	2.43	690	1.57	228	147	1.55
200	1.361	0.42	2.14	718	1.43	223	148	1.50
300	1.385	0.40	1.95	737	1.35	219	149	1.47
400	1.409	0.38	1.80	755	1.25	217	150	1.44
600	1.454	0.34	1.56	789	1.10	215	152	1.41
				T=1300 K				
11.8	1.238 / 0.017	0.61	3.7	621	2.09	247	142	1.74
50	1.252	0.56	3.3	636	1.97	239	142	1.68
100	1.272	0.51	3.0	654	1.84	233	143	1.62
200	1.301	0.45	2.5	685	1.64	224	144	1.55
300	1.328	0.42	2.3	707	1.51	220	145	1.51
400	1.354	0.39	2.1	727	1.40	217	146	1.49
600	1.404	0.36	1.8	765	1.22	215	148	1.45

Table II. (cont.).

$P\cdot10^{-5}$, Pa	$\rho\cdot10^{-3}$, kg m^{-3}	$\alpha_P\cdot10^3$, K^{-1}	$k_T\cdot10^9$, Pa^{-1}	U, m s^{-1}	$k_S\cdot10^9$, Pa^{-1}	c_P, J kg^{-1} K^{-1}	c_V, J kg^{-1} K^{-1}	γ
				T=1400 K				
18.6	1.163 / 0.025	0.71	4.9	578	2.39	260	137	1.89
50	1.179	0.64	4.4	593	2.24	249	138	1.81
100	1.204	0.57	3.8	615	2.10	238	139	1.72
200	1.240	0.49	3.1	650	1.81	227	140	1.62
300	1.271	0.44	2.7	675	1.65	221	141	1.57
400	1.299	0.41	2.4	699	1.51	217	142	1.54
600	1.354	0.37	2.0	741	1.30	214	144	1.49
				T=1500 K				
27.6	1.085 / 0.036	0.83	6.7	533	3.24	277	135	2.06
50	1.101	0.74	5.9	546	3.05	262	135	1.94
100	1.131	0.64	4.9	571	2.71	246	136	1.81
200	1.175	0.53	3.8	613	2.26	231	137	1.69
300	1.211	0.47	3.2	643	2.00	223	138	1.61
400	1.244	0.43	2.8	670	1.79	219	139	1.57
600	1.305	0.38	2.2	717	1.49	213	141	1.51
				T=1600 K				
38.8	1.000 / 0.051	1.0	9.6	486	4.23	298	132	2.26
50	1.010	0.93	8.8	494	4.06	288	133	2.17
100	1.052	0.73	6.6	526	3.44	256	134	1.92
200	1.108	0.59	4.8	575	2.73	237	135	1.76
300	1.149	0.51	3.9	610	2.34	227	136	1.67
400	1.187	0.46	3.3	640	2.06	221	137	1.62
600	1.256	0.40	2.6	693	1.66	216	138	1.57

Table II (concl.).

$P\cdot10^{-5}$, Pa	$\rho\cdot10^{-3}$, kg m^{-3}	$\alpha_P\cdot10^{3}$, K^{-1}	$k_T\cdot10^{9}$, Pa^{-1}	U, m s^{-1}	$S\cdot10^{9}$, Pa^{-1}	c_P, J kg^{-1} K^{-1}	c_V, J kg^{-1} K^{-1}	γ
				T=1700 K				
52.2	0.905 / 0.072	1.3	15.3	435	5.84	347	132	2.62
100	0.965	0.95	10.0	477	4.55	293	132	2.20
200	1.036	0.66	6.2	535	3.37	248	132	1.86
300	1.086	0.55	4.8	576	2.77	234	133	1.75
400	1.128	0.50	4.0	609	2.39	227	134	1.68
600	1.206	0.42	3.0	669	1.85	220	136	1.62
				T=1800 K				
67.8	0.789 / 0.114	2.3	41.0	–	–	–	–	–
100	0.857	1.5	19.0	–	–	–	–	–
200	0.957	0.78	8.6	492	4.32	273	138	1.98
300	1.020	0.61	6.0	542	3.34	242	134	1.80
400	1.067	0.54	5.0	577	2.82	234	133	1.76
600	1.154	0.46	3.5	645	2.08	227	134	1.70
				T=1900 K				
85.8	0.614 / 0.207	7.1	230	–	–	–	–	–
100	0.703	3.1	62.0	–	–	–	–	–
200	0.877	0.95	12.0	444	5.78	315	152	2.08
300	0.954	0.67	7.6	507	4.08	256	137	1.87
400	1.004	0.60	6.2	545	3.35	245	133	1.84
600	1.100	0.50	4.2	619	2.37	234	131	1.78
				T=2000 K				
100	0.189	9.2	470	–	–	–	–	–
200	0.792	1.2	19.0	–	–	–	–	–
300	0.888	0.75	9.8	470	5.14	269	140	1.92
400	0.940	0.66	7.7	510	4.09	257	136	1.88
600	1.045	0.54	5.0	593	2.72	240	131	1.84

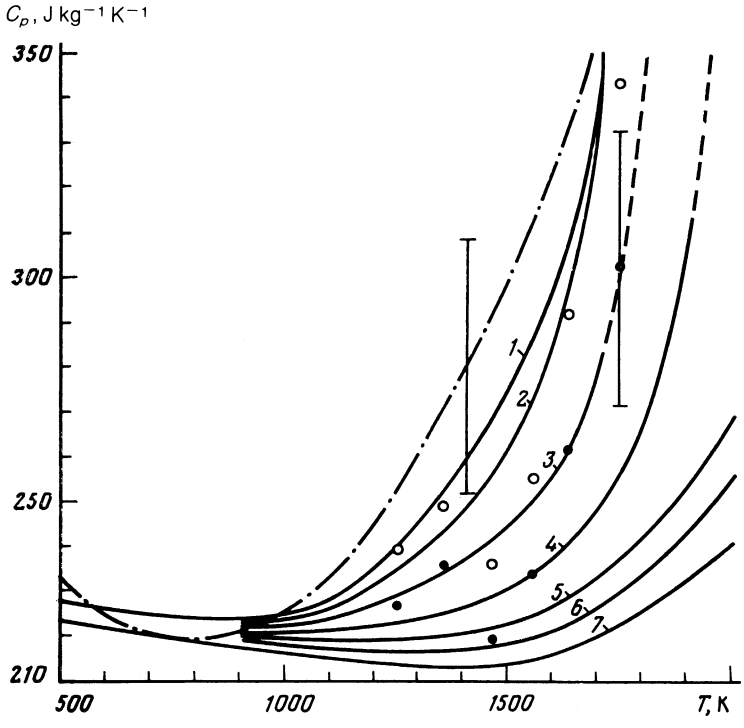

FIG. 4. Specific heat of liquid cesium at constant pressure: 1—on the saturation curve; 2—for $P = 5$ MPa; 3—for $P = 10$ MPa; 4—for $P = 20$ MPa; 5—for $P = 30$ MPa; 6—for $P = 40$ MPa; 7—for $P = 60$ MPa. Broken traces indicate extrapolations, chain curves are defined on the saturation curve;[24] ○ and ● indicate experimental points[25] at pressure of 6 and 9 MPa, respectively.

this function. An example is the virial form used for the EOS of nearly collisionless gases. In the case of liquids and dense gases, no such theory is available, so the experimental data were reduced by a local smoothing technique,[22] using the algorithm described by Vargaftik *et al.*[23] This method has the advantage that there is no need to develop a global prescription for the approximation function, while the derivatives can still be found fairly accurately. The accuracy with which they can be calculated depends primarily on the quality of the data, whereas with a single functional approximation it also depends strongly on the choice of that function.

The rms errors in approximating the EOS and sound speed were 3×10^{-4} g cm^{-3} and 0.8 m s^{-1}, respectively. The specific heat was calculated from

$$C_P=\alpha_P^2TU^2(\gamma-1)^{-1},$$

with

$$\gamma=k_T/k_S=\rho U^2k_T.$$

Table II gives the smoothed values of the thermodynamic properties of liquid cesium. The first line of subcritical isotherms corresponds to the saturated state. The densities of the coexisting liquid and vapor are separated with a horizontal rule. The value of the saturation pressure was taken from Ref. 16. The errors in the tabulated quantities are as follows: $\delta\rho$ varies from 0.2% ($\rho\geqslant1.5$ g cm^{-3}) to 1% ($\rho\leqslant0.02$ g cm^{-3}); $\delta\alpha_P = 1$–3%; $\delta k_T\approx2$–5%; $\delta U\approx0.6$%; $\delta k_S\approx1.5$%; δC_P varies from 15% at $\rho\approx1.7$ g cm^{-3} to 11% at $\rho\approx0.9$ g cm^{-3}; $\delta C_V\approx16$–17%; $\delta\gamma\approx2$–5%.

In Fig. 4 the specific heat C_P is plotted as a function of temperature for several pressures; also shown are values of C_P takes from the literature.[24,25] The evident agreement between the present results and those published previously provides some assurance that our experimental data are consistent and the method with which we reduced them is valid.

5. DISCUSSION

Critical region of cesium. In Fig. 5 we plot $\Delta\rho=(\rho_L^s-\rho_V^s)/2\rho_c$, $\Delta\rho_L=(\rho_L^s-\rho_c)/\rho_c$, and $\Delta\rho_V=(\rho_c-\rho_V^s)/\rho_c$ as functions of $t=(T_c-T)/T_c$, where ρ_L^s and ρ_V^s are the densities of the coexisting liquid and vapor phases. For $7\times10^{-2}\geqslant t\leqslant9\times10^{-3}$ we have $\beta_{LV}=0.40\pm0.01$, $\beta_L=0.44\pm0.01$ and $\beta_V=0.34\pm0.01$, where β_{LV}, β_L, and β_V are the respective exponents on the coexistence curve. In dielectric liquids the corresponding traces have a single power-law behavior with exponent $\beta\approx1/3$, beginning roughly at the same peak values of t (Ref. 26). Our results on the specific heat at constant volume imply that these values of t are associated with well-developed fluctuations, whose properties have to be analyzed in terms of the theory of critical phenomena: the "fluctuational" growth of C_V for liquid cesium in the saturated state begins at $t\approx0.1$ (cf. Fig. 8 below). In argon the rise in C_V also begins at $t\approx0.1$ (Ref. 27).

In the neighborhood of the critical point we can write

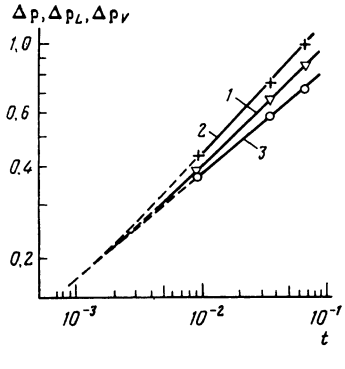

FIG. 5. Coexistence curves for cesium in normalized coordinates (log–log plots); 1—$\Delta\rho\sim t^{0.41}$; 2—$\Delta\rho_L\sim t^{0.44}$; 3—$\Delta\rho_V\sim t^{0.34}$.

expressions for $\Delta\rho_L$ and $\Delta\rho_V$ in the form[28]

$$\Delta\rho_L = B_0 t^{\beta} + B_1 t^{\beta+\varepsilon} + D_0 t^{1-\alpha} + D_1 t + D_2 t^{1-\alpha+\varepsilon} + \ldots, \quad (1)$$

$$\Delta\rho_V = B_0 t^{\beta} + B_1 t^{\beta+\varepsilon} - D_0 t^{1-\alpha} - D_1 t - D_2 t^{1-\alpha+\varepsilon} + \ldots, \quad (2)$$

where β and α are the critical exponents for the coexistence curve in the specific heat at constant volume. Theoretical estimates[29-31] yield values of α and β close to 0.11 and 0.3, respectively ($\varepsilon \approx 0.5$; see Refs. 28, 31).

Although fluctuations affect the equilibrium properties of metallic and dielectric systems noticeably for $t \leqslant 0.1$, it is possible that this influence may develop differently in metals and in dielectrics. In dielectrics in Hamiltonian has to a considerable extent become scale-invariant even for $t \leqslant 5-8\times10^{-2}$, so that the coexistence curve can be accurately approximated by the first term of expressions (1) and (2) (Refs. 33, 34). In view of the specific form of the metallic coupling, particularly the strong density dependence of the interionic interaction, the loss the individual features in the Hamiltonian occurs closer to the critical point in a metallic system. It is possible that for $10^{-3} \leqslant t \leqslant 10^{-1}$ the Ginzburg parameter satisfies $\mathrm{Gi} \sim t$ (i.e., $\mathrm{Gi} \sim \bar{r}^6/r_0^6$) in liquid cesium, where r_0 is the interaction radius and $\bar{r}$ is the average interparticle separation.[35] This implies that at such temperatures the second and higher terms of Eq. (1) exert a perceptible influence,[36] and the asymptotic region shifts in the direction of smaller t.

The closeness of β_V and the theoretical value $\beta \approx 1/3$ allows us to extrapolate the measured values of $\Delta\rho$, $\Delta\rho_L$, and $\Delta\rho_V$, as shown by the broken traces in Fig. 5. Accordingly, the upper bound on the values of t for which the liquid and vapor branches of the coexistence curve can be described by the same power-law dependence (close to 1/3) is two orders of magnitude smaller than in dielectric liquids, which agrees with the assumptions made by Mott.[37] A further peculiarity of the peak of the coexistence curve compared with that of dielectric liquids is found in the big difference in the asymptotic regions for the liquid and vapor branches.

The observed symmetry in the cesium phase diagram near the critical point is undoubtedly connected with the difference in the interaction between particles in liquid and in vapor, which persists under these conditions. Consequently, Fig. 5 serves to confirm that the metal-nonmetal transition in cesium occurs close to the critical ($t \leqslant 10^{-3}$), which is consistent with the available electrical-conductivity data.[38]

Figure 6 displays traces of $\Delta\rho_L$ and $\Delta\rho_V$ vs t for Cs and Rb, taken from Ref. 11, and for Hg, taken from Ref. 1. Evidently the former are entirely consistent with our thesis. The situation is otherwise with mercury. The metal-dielectric transition at a density of 9 g cm^{-3} ($\rho \approx 1.5\rho_c$) causes the peak in the coexistence curve to resemble the ordinary shape ($\beta_L \approx \beta_V \approx 1/3$; cf. Ref. 1).

Average diameter and the law of corresponding states. From Eqs. (1) and (2) it follows that as $T \to T_c$ the average diameter $\rho_d - 1 \equiv (\rho_L^s + \rho_V^s)/2.1 = f(T)$ becomes singular with critical exponent $1-\alpha$ (Ref. 30). As a rule this singularity is not observed for dielectrics. In SF_6 the diameter was observed to undergo a slight curvature close to the critical point ($t \leqslant 10^{-5}$), where the gravitational field exerts a perceptible influence on the results of the measurements.[39]

In many experimental investigations of metal phase diagrams it was assumed *a priori* that the diameter is rectilinear. (This is one reason why the old and new cesium critical parameters differ; cf. Table I.) Deviations from this law were first observed by Kikoin and Senchenkov[40] in studies of the equation of state of mercury and confirmed by Kikoin *et al.*[1] Jungst *et al.*[11] observed curvature in the average diameter of cesium and rubidium, also confirmed in the present work.[1)]

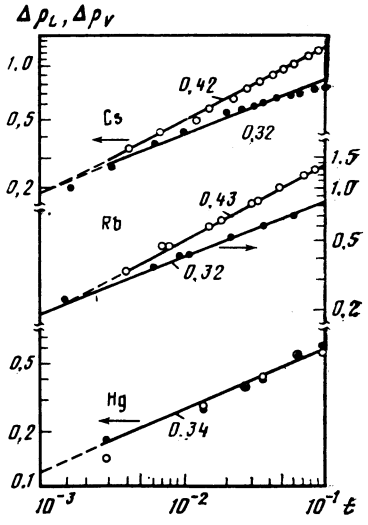

FIG. 6. Coexistence curve for cesium and rubidium[11] and mercury:[1] ○—$\Delta\rho_V$; ●—$\Delta\rho_L$. The numbers labelling the traces are the values of the corresponding exponents.

Vaks *et al.*[35] treated the curvature of the average diameter of the phase diagram of cesium and rubidium[11] as a singularity manifested by anomalously large values of the corresponding terms of the expansions (1), (2) in metals. Without ruling out this possibility, we note that a purely "singular" explanation of this phenomenon runs into difficulty because the curvature in the diameter occurs fairly far from the critical point ($t \approx 0.4$), where fluctuations are negligible.

Unlike the situation in dielectrics, the coexistence curve in metals separates systems with qualitatively different interactions: Van der Waals interactions between the vapor molecules and metallic between ions in the liquid. Obviously one would not expect metals and dielectrics to be similar thermodynamically. The specific form of the differences must depend on the valence electron states defined by the interactions between ions in the metallic liquid.

Figure 7 displays plots for eight dielectric liquids from the work of Guggenheim,[41] along with data for mercury[1] and cesium. It is clear that the basic differences between the phase diagrams of metals and those of dielectrics are associated with the liquid branches. For the metals the average diameters are curved, in opposite directions for mercury (valence 2) and cesium (valence 1).

Anisimov and Zaprudskiĭ[42] have shown that the curvature of the average diameter in the mercury phase diagram[1] can be explained in terms of an interaction between the order parameters of the liquid–gas and metal–dielectric transitions.

Strong asymmetry in the coexistence curve and related curvature of the average diameter have also been observed in other systems with long-range coupling: metal-ammoniate

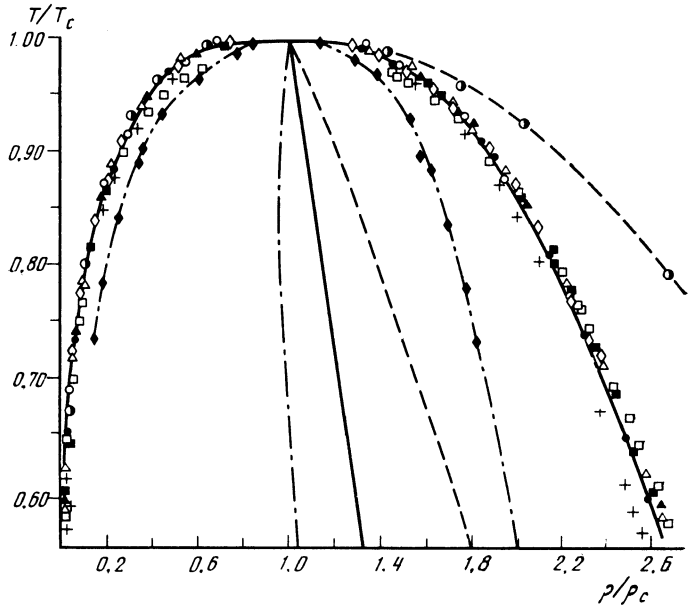

FIG. 7. Phase diagrams of the dielectric liquids: Ne (+), Ar(●), Kr(■), Xe(×), N_2(△) O_2(▲) CO(□), CH_4 (○; Ref. 40), Hg(◆, Ref. 1), and Cs(◑).

solutions and electron-hole in semiconductors.[43] This permits us to assert that the law of rectilinear diameters is valid only for systems with short-range coupling, including (among others) simple dielectric liquids.

Cesium specific heat at constant volume. Because of technical problems, specific heats at constant volume are not measured directly for liquid metals. The available data on C_V (cf., e.g., Novikov *et al.*[19]) were calculated by means of well known thermodynamic relationships from various combinations of experimental data on EOS, sound speed, and C_P. Using data from different sources can give rise to qualitatively different temperature dependence in C_V, e.g., the presence or absence of a minimum at low temperatures. A similar situation is found on the theoretical side.[44–46]

Since calculations of C_V are highly sensitive to errors in the initial experimental data, it is important that these data be as accurate as possible and that relative error be as small as possible, i.e., that the measurements be carried out consistently with the same thermometers and pressure gauges. The experimental data of the present work meet this requirement fully. Figure 8 shows C_V for liquid cesium as a function of temperature and pressure. It is seen that C_V decreases monotonically from $\sim 3R$ near the melting point to $2R$ in the neighborhood of the critical point, which agrees with the qualitative picture that translational oscillation modes are gradually lost as one moves away from the melting point.[47] An estimate based on the free-electron model of the contribution of the electron heat capacity to the conductivity lies slightly outside the error bars on the values of C_V we have obtained at the lowest temperatures studied. We regard this as an indication of the deficiencies of the model under these conditions.

6. CONCLUSIONS

We summarize the basic conclusions drawn from this study.

1. High-accuracy measurements of the equation of state and speed of sound in cesium have enabled us to obtain improved values of the critical parameters and to compile detailed tables of the thermodynamic properties of this metal over the whole temperature range in which it is found in the liquid phase.

2. We have revealed ways in which the phase diagram of cesium differs from those of simple nonconducting liquids:

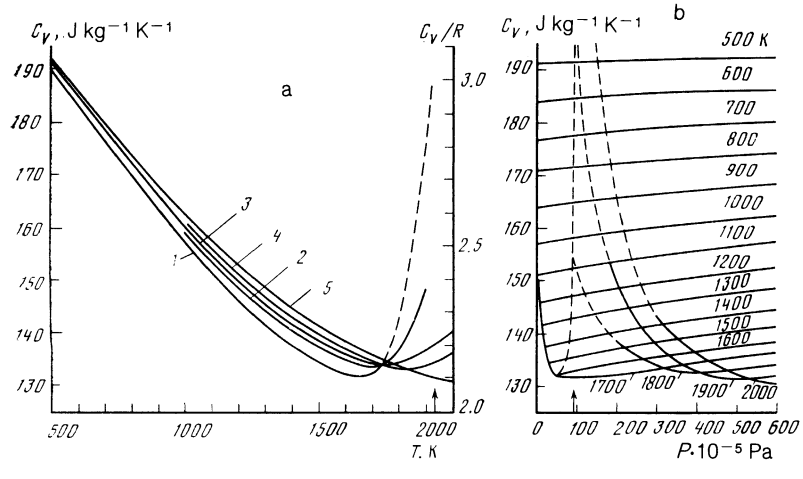

FIG. 8. Cesium specific heat at constant volume as a function (a) of temperature and (b) of pressure: 1—on the saturation curve; 2—for $P = 20$ MPa; 3—for $P = 30$ MPa; 4—for $P = 40$ MPa; 5—for $P = 60$ MPa. The temperature and pressure at the critical point are indicated by arrows. Broken lines indicate the portions constructed by estimating the second derivatives of the EOS.

the critical region of cesium is two orders of magnitude smaller than that of dielectrics, and the breakdown of the law of rectilinear diameters in metal systems has been confirmed.

3. The cesium specific heat at constant volume has been shown to decrease monotonically from $\sim 3R$ near the melting point to $\approx 2R$ at the critical point, exhibiting no minimum up to 1700 K.

I am deeply grateful to N. B. Vargaftik, D. I. Arnol'd, S. P. Naurzakov, E. B. Gel'man, and E. V. Grodzinksiĭ for support and assistance in the course of this work, and to V. G. Vaks for valuable comments.

[1)] In Ref. 11 the critical exponent of the diameter was estimated to be 0.87 ± 0.03 for cesium and 0.86 ± 0.03 for rubidium. A similar estimate based on our data yields 0.94 ± 0.03.

[1]I. K. Kikoin, A. P. Senchenkov, S. P. Naurzakov, and É. B. Gel'man, Preprint IAÉ-2310, Moscow (1973).
[2]J. M. Hochman and C. F. Bonilla, Proc. 3rd Symp. Thermophys. Properties, ASME, New York (1965), p. 122.
[3]I. G. Dillon, P. A. Nelson, and B. S. Swanson, J. Chem. Phys. **44**, 4229 (1966).
[4]H. Renkert, F. Hensel, and E. U. Frank, Phys. Lett. A **30**, 1944 (1969); Ber. Bunsenges. Phys. Chem. **75**, 507 (1971).
[5]V. A. Alekseev, V. G. Ovcharenko, Yu. F. Ryzhkov, and A. P. Senchenkov, Pis'ma v ZhETF **12**, 306 (1970) [JETP Lett. **12**, 207 (1970)].
[6]Yu. S. Korshunov, A. P. Senchenkov, É. I. Asinovskiĭ, and A. T. Kunavin, Teplofiz. Vys. Temp. **8**, 1288 (1970); Yu. S. Korshunov, S. P. Vetchinin, A. P. Senchenkov, and É. I. Asinovskiĭ, Teplofiz. Vys. Temp. **13**, 517 (1975).
[7]I. L. Silver and C. F. Bonilla, Proc. 5th Symp. Thermophys. Properties, ASME, New York (1970), p. 461.
[8]G. F. Oster and C. F. Bonilla, Proc. 5th Symp. Thermophys. Properties, ASME, New York (1970), p. 468.
[9]S. Das Gupta, V. Bhise, D. W. Stuteville *et al.*, Proc. 6th Symp. Thermophys. Properties, ASME, New York, (1970), p. 387.
[10]G. Franz, W. Freland, and F. Hensel, J. Physique Col. C8, Suppl. 8, **41**, 70 (1970).
[11]S. Jungst, B. Knuth, and F. Hensel, Phys. Rev. Lett. **55**, 2160 (1955).
[12]N. B. Vargaftik, V. F. Kozhevnikov, and V. A. Alekseev, in *Handbook of Thermodynamic and Transport Properties of Alkali Metals*, ed. R. W. Ohse, Blackwell, Oxford (1985), p. 471.
[13]N. B. Vargaftik, V. F. Kozhevnikov, and P. N. Ermilov, High Temp.-High Press. **16**, 233 (1984).
[14]N. B. Vargaftik, E. B. Gelman, V. F. Kozhevnikov, and S. P. Naurzakov, Proc. 11th AIRAPT Inter. Conf. Naukova Dumka, Kiev (1989), vol. 1, p. 57.
[15]V. F. Kozhevnikov and P. N. Ermilov, Prib. Tekh. Eksp. (1), 209 (1982).
[16]M. A. Pokrasin, V. V. Roshchupkin, L. P. Fokin, and N. E. Khandomirova, *Teplofizicheskaya svoĭstva veshchestv i materialov*, Izd. Standartov, Moscow **19**, 33 (1983).
[17]N. B. Vargaftik, L. D. Volyak, and V. G. Stepanov, in *Handbook of Thermodynamic and Transport Properties of Alkali Metals*, ed. R. W. Ohse, Blackwell, Oxford (1985), p. 641.
[18]I. I. Novikov, V. V. Roshchupkin, Yu. S. Trelin *et al.*, *Skorost'zvuka v zhidkikh shchelochnykh metallakh: obzory po teplofizicheskim svoĭstvam veshchestv (Speed of Sound in Liquid Alkali Metals: Reviews of Material Thermophysical Properties)*, IVTAN, Moscow **6**(32), 65 (1981).
[19]I. I. Novikov, V. V. Trelin, and T. A. Tsyganova *et al.*, Teplofiz. Vys. Temp. **8**, 450 (1970).
[20]D. I. Arnol'd, A. M. Gordenko, P. N. Ermilov *et al.*, Prib. Tekh. Eksp. (5), 167 (1985).
[21]N. B. Vargaftik, D. I. Arnold, A. M. Gordenko *et al.*, Inter. J. Thermophys. **7**, 821 (1985).
[22]C. Lanczos, *Applied Analysis*, Prentice-Hall, Englewood Cliffs, NJ (1957) [Russ. transl. Nauka, Moscow (1963)].
[23]N. B. Vargaftik, E. B. Gelman, V. F. Kozhevnikov, and S. P. Naurzakov, Inter. J. Thermophys. **10** (1989).
[24]P. I. Bystrov, D. N. Kagan, G. A. Krechetova, and É. É. Shpil'raĭn, *Zhidkometallicheskie teplonositeli teplovykh trub i énergeticheskikh ystanovok (Liquid-Metal Working Media in Heat Pipes and Power-Generation Machinery)*, Nauka, Moscow (1988).
[25]V. A. Alekseev, L. A. Blagonravov, and L. P. Filippov, J. Physique Col. C8, Suppl. 8, **41**, 607 (1980).
[26]M. A. Anisimov, *Kritcheskie yavleniya v zhidkostyak i zhidkikh kristallakh (Critical Phenomena in Liquids and Liquid Crystals)*, Nauka, Moscow (1987).
[27]J. Thoen, E. Vangeel, and W. Van Dael, Physica **45**, 339 (1969).
[28]M. Ley-Koo and M. G. Green, Phys. Rev. A**16**, 2483 (1977).
[29]J. Kogut and K. Wilson, *The Renormalization Group and the ε-Expansion*, Phys. Rep. **12**, 75 (1974) [Russ. transl. Mir, Moscow (1975)].
[30]A. Z. Potashinskiĭ and V. L. Pokrovskiĭ, *Fluktuatsionnaya teoriya fazovykh perekhodakh (Fluctuation Theory of Phase Transitions)*, Nauka, Moscow (1982).
[31]G. A. Baker, B. G. Nichel, and D. I. Meiron, Phys. Rev. B**17**, 1365 (1978).
[32]J. M. H. Levelt-Sengers, J. S. Gallagher, F. W. Bonfour, and J. V. Sengers, Proc. 8th Symp. Thermophys. Properties, Ed. J. V. Sengers, ASME, New York (1982), vol. 1, p. 468.
[33]A. V. Voronel', V. G. Gorbunova, V. A. Smirnov *et al.*, Zh. Eksp. Teor. Fiz. **63**, 964 (1972) [Sov. Phys. JETP. **36**, 505 (1973)].
[34]P. R. Roach, Phys. Rev. **170**, 213 (1968).
[35]V. G. Vaks, A. I. Larkin, and S. A. Pikin, Zh. Eksp. Teor. Fiz. **51**, 361 (1966) [Sov. Phys. JETP **24**, 240 (1967)].
[36]R. E. Goldstein and N. W. Ashcroft, Phys. Rev. Lett. **55**, 2164 (1985).
[37]N. F. Mott, *Metal-Insulator Transition*, Comtemp. Phys. **14**, 401 (1973) [Russ. transl. Nauka, Moscow (1979)].
[38]F. Hensel, Proc. 8th Symp. Thermophys. Properties, Ed. J. V. Sengers, ASME, New York (1982), vol. 2, p. 151.
[39]D. Yu. Ivanov, L. A. Makarevich, and O. N. Sokolova, Pis'ma v ZhETF **20**, 272 (1974) [JETP Lett. **20**, 121 (1974)]; D. Yu. Ivanov and V. K. Fredyanin, Preprint OIYaI P4-8430, Dubna (1974).
[40]I. K. Kikoin and A. P. Senchenkov, Fiz. Metal. Metalloved. **24**, 843 (1967).
[41]E. A. Guggenheim, J. Chem. Phys. **13**, 253 (1945).
[42]M. A. Anisimov and V. M. Zaprudskiĭ, DAN SSSR **245**, 78 (1979) [Sov. Phys. Doklady **24**, 187 (1979)].
[43]G. A. Thomas, J. Phys. Chem. **88**, 3749 (1984).
[44]V. P. Onishchenko, PhD Dissertation, ITIKhPO, Odessa (1973).
[45]G. S. Aslanyan, PhD Dissertation, IVTAN, Moscow (1977).
[46]A. M. Bratkovskiĭ, DSc Dissertation, IAÉ, Moscow (1982).
[47]T. E. Faber, *Introduction to the Theory of Liquid Metals*, Cambridge Univ. Press (1972).

Translated by David L. Book